Ecological Modelling 316 (2015) 111–121

Contents lists available at ScienceDirect

Ecological Modelling

journal homepage: www.elsevier.com/locate/ecolmodel

Modelling the spread of the invasive alga *Codium fragile* driven by long-distance dispersal of buoyant propagules

Karine Gagnon[a,*], Stephanie J. Peacock[b], Yu Jin[c,1], Mark A. Lewis[b,c]

[a] *Département de biologie, Université Laval, 1045, avenue de la Médecine, Québec, QC G1V 0A6, Canada*
[b] *Department of Biological Sciences, University of Alberta, Edmonton, Alberta T6G 2E9, Canada*
[c] *Department of Mathematical and Statistical Sciences, University of Alberta, Edmonton, Alberta T6G 2G1, Canada*

ARTICLE INFO

Article history:
Received 30 November 2014
Received in revised form 29 July 2015
Accepted 8 August 2015
Available online 1 September 2015

Keywords:
Individual-based model
Invasive algae
Dispersal
Codium fragile
Secondary spread

ABSTRACT

The secondary spread of an invasive species after initial establishment is a major factor in determining its distribution and impacts. Determining and understanding the factors driving this secondary spread is therefore of great importance to manage and predict invasions. In this study we constructed an individual-based model for the spread of the invasive green alga *Codium fragile* ssp. *fragile* along a straight coastline, in order to understand the factors governing spreading speed. *Codium* can spread locally through non-buoyant propagules, while long-distance dispersal depends on the wind-driven dispersal of buoyant fragments. Since fragment buoyancy is determined by light conditions, we first modelled the buoyancy of fragments, yielding a dispersal time dependent on light conditions. We then used this dispersal time, along with empirical wind speeds and directions to calculate a dispersal kernel for fragments. Finally, we incorporated this dispersal kernel into a population growth model including survival rate and fragmentation rate, to calculate a population spreading speed. We found that under current environmental conditions along the east coast of Canada, (the northernmost front of this invasion) further spread towards the northeast is possible but limited (only 4 km yr^{-1}). However, a sensitivity analysis showed that environmental shifts associated with climate change, such as more variable winds and increased disturbances that cause fragmentation, have the potential to increase spreading speed and particularly northward spread.

1. Introduction

The secondary spread of an invasive species after its initial introduction is of great importance in determining the final distribution and impact of the species (Parker et al., 1999; Molnar et al., 2008). However, secondary spread is difficult to predict as it rarely occurs at a constant speed. Rather, it involves periods of rapid spread over long distances due to movement patterns of vectors (e.g. human activity; Padilla et al., 1996) or favourable environmental conditions (McQuaid and Phillips, 2000), interspersed with long periods of little to no spread. These long-distance dispersal events ("jump dispersal") are often anthropogenically driven (Blakeslee et al., 2010), but can also occur naturally (e.g. Forrest et al., 2000; Stewart, 2006). In addition, dispersal potential and survival within a species can vary widely among individuals (or propagules) and with environmental conditions. Predicting the spread of an invasive species is thus a difficult task, but understanding which factors determine secondary spread is key to managing the impacts of invaders on ecosystems (Vander Zanden and Olden, 2008).

Mathematical models based on available data are useful tools for understanding and predicting the secondary spread of invasive species. A variety of such models have been proposed to explain species spread, beginning with reaction-diffusion models (Fisher, 1937; Skellam, 1951) and variations thereof (Hengeveld, 1989). However, these models do not take into account long-distance or jump dispersal events, which may be the most important factor in determining invasion rates (Hastings et al., 2005). More recently, individual-based models (IBMs) have been developed which can be used to calculate dispersal kernels including low probability long-distance dispersal events (Fennell et al., 2012). These models incorporate stochastic ("random") components to account for differences in the conditions experienced by individual propagules (DeAngelis and Mooij, 2005). Markov Chain Monte Carlo (MCMC)

* Corresponding author. Current address: Department of Biology, University of Turku, FI-20014 Turun Yliopisto, Finland. Tel.: +358 333 5011.
E-mail addresses: karine.gagnon@utu.fi (K. Gagnon), stephanie.peacock@ualberta.ca (S.J. Peacock), yjin6@unl.edu (Y. Jin), mark.lewis@ualberta.ca (M.A. Lewis).
[1] Current address: Department of Mathematics, University of Nebraska-Lincoln, Lincoln, NE 68588-0130, USA.

http://dx.doi.org/10.1016/j.ecolmodel.2015.08.011
0304-3800/

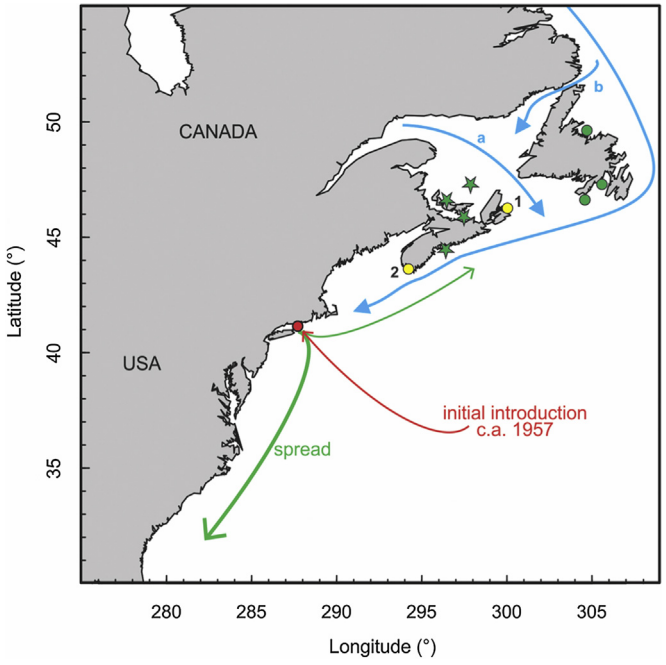

Fig. 1. Spread of *Codium fragile* in the NW Atlantic. The red line indicates the initial introduction Long Island Sound the 1950s (likely from Europe). The green arrows show the general direction of potential spread by buoyant fragments as predicted by our model, with the thickness of the lines representing the magnitude of this spread towards the southwest and northeast. The green star indicates the northernmost populations of *Codium* in eastern Canada prior to 2010, while the green circles indicate further spread to Newfoundland since 2012. Major oceanic currents are indicated in blue: (a) the Gaspé current flowing southeast through the Gulf of St. Lawrence, and (b) the Labrador current flowing around Newfoundland and down the eastern coast of North America. Points in yellow mark from where (1) weather (Sydney, Nova Scotia) and (2) wind (Baccaro Point, Nova Scotia) data used in the simulations was obtained. (For interpretation of the references to colour in this figure legend, the reader is referred to the web version of this article.)

methods can be used to simulate an IBM repeatedly and obtain population-level statistics that account for variability in physical and environmental processes among individuals (Gardner and Gustafson, 2004).

In this study, we used a mechanistic IBM to estimate the dispersal kernel in an integro-difference model of population growth and spread (Lewis et al., 2006), and determine the most important factors controlling population spread along a hypothetical straight coastline. We applied the model to determine the dispersal potential and spreading speed of the invasive green alga *Codium fragile* spp. *fragile* (formerly ssp. *tomentosoides*, hereafter *Codium*) in the NW Atlantic, and compared this spread to the actual recorded spread (Fig. 1). Considered a notorious invader (Trowbridge, 1998; Molnar et al., 2008) due to its capacity for spread and impacts on benthic communities (e.g. Garbary et al., 2004; Scheibling and Gagnon, 2006), *Codium* was first recorded in eastern North America in 1957 in Long Island Sound (Bouck and Morgan, 1957), likely arriving from Europe through ballast water or aquaculture transfers (Chapman, 1999). Over 50 years, it has spread northwards to the Gulf of St. Lawrence where it has been present since approximately 1996 (Garbary et al., 1997). Spreading speed has occurred in jumps and starts (Chapman, 1999) implying a form of stratified diffusion (Shigesada et al., 1995) with long-distance dispersal events driving the invasion front (Neubert and Caswell, 2000).

Invasive *Codium* subspecies can reproduce asexually through parthenogenesis (Prince and Trowbridge, 2004) or fragmentation (Trowbridge, 1998). Fragmentation can occur spontaneously in cold waters (Fralick and Mathieson, 1972) or mechanically through natural (e.g. storms and ice scouring) and anthropogenic disturbances (West et al., 2007). Stratified diffusion in *Codium* is thus likely due to the combined dispersal of asexually-produced propagules, and non-buoyant and buoyant fragments. Parthenogenesis and non-buoyant fragments increase local population density buoyant fragments can disperse many kilometres travelling via wind-driven surface currents before settling and forming new populations (Gagnon et al., 2011, 2015).

The use of buoyant fragments for long-distance dispersal is not unique to *Codium*; other macroalgae such as the invasive *Sargassum muticum* possess specialized air vesicles to keep them afloat (Deysher and Norton, 1982; Stewart, 2006). However, unlike many species of buoyant algae, *Codium* lacks specialized structures for buoyancy and instead relies on oxygen bubbles trapped within the thallus (Dromgoole, 1982). As these oxygen bubbles may leak out of the thallus over time, *Codium* must produce oxygen via photosynthesis to maintain positive buoyancy, providing an interesting link between sunlight and the dispersal potential of this alga (Gagnon et al., 2011).

We developed an IBM for the long-distance dispersal and interannual spread of *Codium* in order to determine important factors influencing spread. An estimate of the dispersal kernel of buoyant fragments was determined through independent simulations of the dispersal of many fragments. These simulations incorporated physiological processes and environmental conditions determining the period of buoyancy, as well as environmental factors affecting the dispersal distance of buoyant fragments due to wind over that period. The dispersal kernel was then used to estimate the stochastic spreading speed of *Codium* along a one-dimensional domain (Neubert et al., 2000), representing a coastline. We applied the model using environmental parameters from the east coast of Canada (the northern front of the invasion), and compared our results to the recorded spread of *Codium* in the NW Atlantic. We then performed a sensitivity analysis to determine which parameters had the greatest influence on the spreading speed of *Codium*. These parameters may be important in determining how changing environmental conditions could affect future spread and management strategies.

2. Methods

2.1. Background

The spread of invasive *Codium* was modelled in a mechanistic framework that included sub-models for sunlight and photosynthesis (Sections 2.2 and 2.3), the buoyancy of fragments (Section 2.4), dispersal times and distances (Sections 2.4 and 2.5) and population spread (Section 2.6), including stochastic components throughout (Fig. 2). For each fragment, we simulated a time series of light intensities, calculated oxygen production given those light intensities, determined the buoyancy of the fragment from the amount of oxygen it contained, and the time at which buoyancy became negative and the fragment sank. We tracked the fragment's wind-driven movement along a one-dimensional domain over the period of positive buoyancy, and the displacement upon sinking was taken to be the fragment's dispersal distance. This algorithm was repeated for 1000 fragments, which we found to be a sufficiently large number to give consistent population-level estimates of spreading speed (see Fig. A1.3). We used the distribution of dispersal distances for these 1000 fragments as an empirical estimate of the dispersal kernel in an integro-difference model of population spread.

We used environmental conditions from in late summer or early autumn in our simulations, as this is when dispersal potential is highest. At that time, fragmentation increases as adult thalli reach maximum size (Bégin and Scheibling, 2003) and rougher autumn

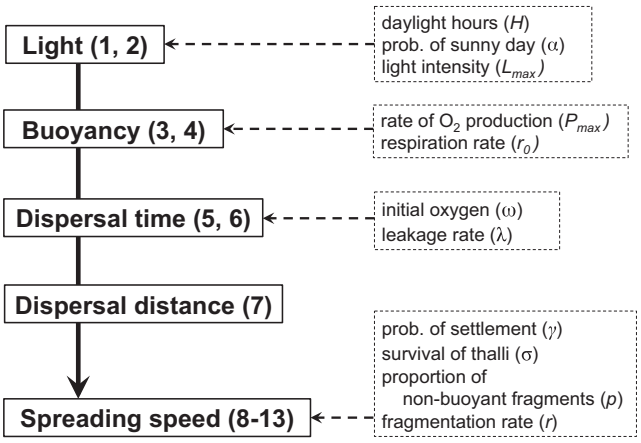

Fig. 2. The model of population spread for *Codium* includes sub-models for light, buoyancy, dispersal time, wind, dispersal distance and spreading speed. Equation numbers are shown in parentheses next to sub-model names in solid boxes, while key parameters for each sub-model are shown with dashed boxes and arrows. The base values for these parameters are given in Table 1.

weather breaks thalli, but there are still enough daylight hours for fragments to remain buoyant for several days to weeks. We used environmental data from the eastern coast of Nova Scotia, Canada (Environment Canada, 2015a, 2015b; Fig. 1), as this area was near the northern front of the *Codium* invasion in the NW Atlantic at the time of the study (Simard et al., 2007), with conditions relevant for predicting further spread of this invader northward. *Codium* has since spread further north (Matheson et al., 2014; Fig. 1), allowing us the opportunity to compare our predictions to both historical and recent spread along the northeastern coast of North America.

2.2. Light intensity

Codium fragments continue to photosynthesize after being detached from the substrate, continually producing oxygen that is trapped in the medulla and keeping the fragments buoyant. The long-distance dispersal of *Codium* fragments is therefore linked to the intensity and amount of sunlight. Fragments will sink if a series of cloudy days or fewer daylight hours result in lower oxygen production and a net loss of oxygen from the medulla due to respiration and leakage. We explicitly modelled the light intensity over a maximum dispersal period of 60 days. The light intensity $L(t)$ was modelled as a sine curve, shifted so there were H daylight hours with a maximum light intensity L_{max} (Fig. 3A). We report light intensity in units of kilolux (klx). Outside of daylight hours, we set light intensity at 0 klx. The light intensity at t hours was:

$$L(t) = \max\left\{0, \frac{L_{max}}{H-4} \cdot \left(8\sin\left(\frac{\pi t + 6}{12}\right) + H - 12\right)\right\}. \quad (1)$$

We accounted for the stochastic nature of weather by randomly determining the weather each day of the simulation, basing the probability of a sunny day from historical weather data. To do this, we drew a binomial random variable, $z \sim \text{Binom}(\alpha)$, where $z = 1$ dictated a sunny day and $z = 0$ dictated a cloudy day for each day of the simulation. The probability of success for the binomial distribution, α, was the average proportion of days in a month that were sunny from historical weather data for Sydney, NS (Environment Canada, 2015b). As a base value, we considered historical weather for August only (Table 1), but we also considered other months in the sensitivity analyses (Section 2.7). The maximum light intensity for the day was then chosen from a log-normal distribution of light intensities based on whether it was sunny or cloudy (Arnold and Murray, 1980; Gagnon et al., 2011; Fig. 3A and Fig. A1.1):

$$L_{max} \sim \begin{cases} \text{logNormal}(\log(30), 0.2) & \text{if sunny } (z = 1) \\ \text{logNormal}(\log(10), 0.2) & \text{if cloudy } (z = 0) \end{cases} \quad (2)$$

This stochastic algorithm produced a time series of light intensities that increased to different peak intensities each day (Fig. 3B).

2.3. Photosynthesis

Photosynthetic rates in algae generally increase with increasing light intensity to a maximum rate beyond which rates may plateau or even decline due to photosynthetic inhibition (though the latter does not seem to occur in *C. fragile*; Arnold and Murray, 1980). We modelled net photosynthesis (i.e. accounting for respiration) as:

$$O(t) = \frac{mL(t)}{1 + L(t)\left(\frac{m}{P_{max}+r_0}\right)} - r_0 \quad (3)$$

where $O(t)$ is the rate of oxygen production ($\text{cm}^3 \cdot \text{g}$ dry weight of $\text{alga}^{-1} \cdot \text{h}^{-1}$), m is the slope of oxygen production with light intensity at low light intensities, P_{max} is the maximum rate of oxygen production and r_0 is the rate of respiration (Table 1). Using our modelled light intensities from Eq. (1) and empirically estimated parameters

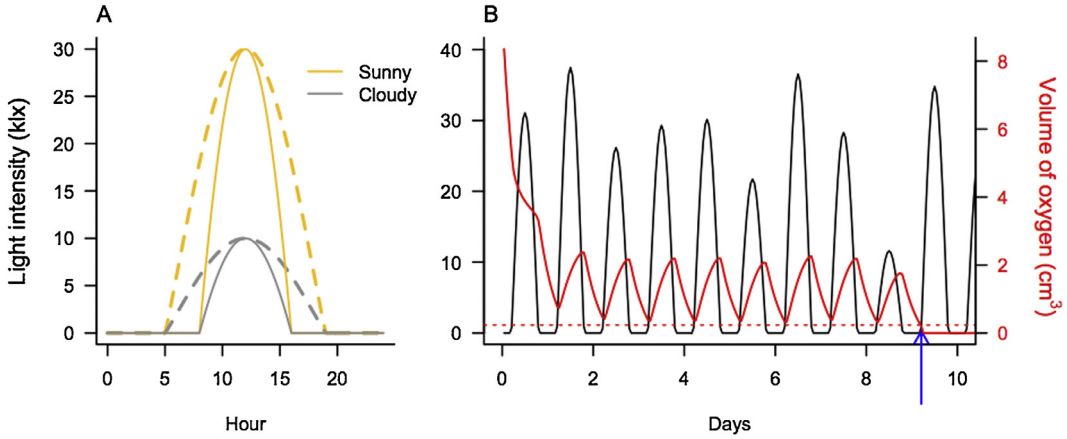

Fig. 3. (A) Example of light intensity on a sunny (gold) or cloudy (grey) day with 8 (solid) or 14 (dashed) hours of daylight. (B) Simulated light intensities over 10 days (black line) and corresponding oxygen volumes (red line, right axis) with base parameters (Table 1). The horizontal dotted red line indicates the critical volume of oxygen below which a fragment will become negatively buoyant in seawater. The time at which this occurs is considered the dispersal time, in this case ~ 9 days (blue arrow). (For interpretation of the references to colour in this figure legend, the reader is referred to the web version of this article.)

Table 1
Parameters and base values for simulations of *Codium fragile* population spread due to the dispersal of buoyant fragments. Equation numbers indicate where the parameters are first mentioned. Parameter values taken from the literature are indicated with a footnote citing the reference.

Eq.	Parameter	Symbol	Base value
	Number of fragments	N	1000
(1)	Number of daylight hours[a]	H	14.33
(2)	Probability of sunny day[a]	α	0.91
	Maximum daily light intensity[b]	L_{max}	$L_{max} \sim \begin{cases} \text{logNormal}(\log(30), 0.2) & \text{if sunny } (z = 1) \\ \text{logNormal}(\log(10), 0.2) & \text{if cloudy } (z = 0) \end{cases}$
(3)	Slope of O_2 production at low light[b]	m	0.88 cm^3 O_2 g dry wt^{-1} h^{-1} klx^{-1}
	Maximum rate of O_2 production[b]	P_{max}	0.40 cm^3 O_2 g dry wt^{-1} h^{-1}
	Respiration rate[b]	r_0	2.16 cm^3 O_2 g dry wt^{-1} h^{-1}
(5a)	Leakage rate	λ	0.1 h^{-1}
(5b)	Proportion of excess O_2 at start	ω	0.8
(8)	Probability of successful settlement	γ	0.01
	Survival of thalli[c]	σ	0.2 yr^{-1}
	Proportion of fragments that are non-buoyant at fragmentation	p	0.5

Source: [a]Environment Canada (2015a); [b]Gagnon et al. (2011); Arnold and Murray (1980); [c]Fralick and Mathieson (1972).

m, r_0 and P_{max} from Arnold and Murray (1980), we simulated the oxygen production within each fragment. We converted the parameter estimates from Arnold and Murray (1980) from units of carbon uptake per gram dry weight of seaweed into the rate of oxygen production per wet weight (see *Supplement A2* for details of how Eq. (3) was parameterized).

2.4. Buoyancy and dispersal time

The buoyancy of a *Codium* fragment was determined by its relative density, i.e., if the density of the *Codium* fragment (ρ_f) was greater than that of the surrounding water (ρ_w) it sank, but if it was less than the density of the water it floated. We considered fragments as cylinders with two sections: the exterior cortex composed of photosynthetic cells and the interior medulla which is made of filaments with hollow spaces in which air bubbles can accumulate (Fig. 4). The total volume of a fragment (V_f) is thus the sum of the volume of the cortex (V_c) and the volume of the medulla (V_m). Dromgoole (1982) found that the density of *Codium* was fairly constant with percent water content at 1.042 g cm^{-3}, which we took to be the density of the cortex (ρ_c). As the medulla can be filled with water (V_w), air (V_a), or some combination, if the densities of water, air (ρ_a), and the cortex are known, the total density of the fragment can therefore be determined by:

$$\rho_f = \frac{\rho_c V_c + \rho_a V_a + \rho_w (V_m - V_a)}{V_f}. \tag{4}$$

Buoyancy is driven by the volume of oxygen (V_a), which depends on the initial volume at fragmentation ($V_a(0)$) and net photosynthesis. The change in the volume of oxygen is described by:

$$\frac{dV_a(t)}{dt} = -\lambda V_a(t) + O(t)(0.05\rho_c V_c), \tag{5a}$$

which can be integrated to give the volume of oxygen at time t:

$$V_a(t) = e^{-\lambda t}\left(V_a(0) + \int_0^t e^{\lambda\tau} O(\tau)(0.05\rho_c V_c)\ d\tau\right), \tag{5b}$$

where λ is the leakage rate of oxygen from the medulla and $O(t)$ is the photosynthetic rate per gram dry weight of seaweed from Eq. (3). Photosynthetic rates were given per gram dry weight of seaweed, and we assumed the ratio of dry weight to fresh weight was 0.05 when simulating oxygen production per fragment (Hwang et al., 2008). As a base value we assumed $\lambda = 0.1\ h^{-1}$, which is an approximate value that produces buoyancy predictions that match data from Gagnon et al. (2011), but we explored this parameter in sensitivity analyses with values from 0 to 0.2 (Section 2.7). When calculating $V_a(t)$, we ensured that we could not have more air than volume of the medulla, or negative volumes ($0 \le V_a(t) \le V_m$). The volume of oxygen needed for the density of the fragment to become equal to that of water can then be calculated as:

$$V_a^* = \frac{V_c(\rho_w - \rho_c)}{\rho_a - \rho_w}. \tag{6}$$

The volume of oxygen within a fragment ($V_a(t)$) was calculated over time from the simulated light intentisities and corresponding oxygen production (Fig. 3B). The initial volume of oxygen is assumed to be greater than V_a^* for buoyant fragments. We considered the dispersal time (T) of a fragment to be the first time at which $V_a(t) \le V_a^*$. We thus assumed that when fragments become negatively buoyant, they cannot return to a positively buoyant state and thus settle. This assumption seems reasonable given that light attentuation in sea water results in exponential decay in the photosynthetically active radiation with depth. The proportion of excess oxygen at fragmentation (ω) is zero if the fragment is neutrally buoyant (i.e., $V_a = V_a^*$) and one if the medulla is completely filled with oxygen (i.e., $V_a = V_m$). Since we were uncertain about this value, we considered a range of values from 0.05 to 1 in a sensitivity analyses (Section 2.7).

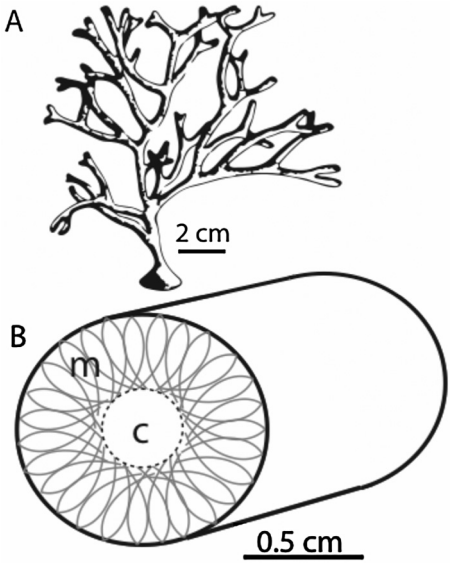

Fig. 4. (A) Structure of a *Codium* thallus and (B) a cross section of a fragment showing the medulla (m) where oxygen is trapped and the cortex (c).

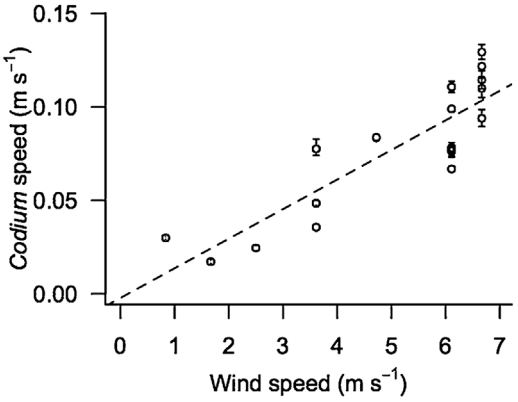

Fig. 5. Relationship between dispersal speed (in the same direction as wind speed) of *Codium* fragments and wind speed for buoyant fragments in the Magdalen Islands (Gagnon et al., 2015). The equation of the line is $y = -0.0022 + 0.0158x$, where the slope ($\beta_1 = 0.0158$) indicates the proportion of the wind speed at which buoyant fragments move.

2.5. Wind and dispersal distance

Buoyant fragments travel along the water surface, and their dispersal is driven by wind. Previous experiments in lagoons of the Magdalen Islands of eastern Canada found a strong correlation between the distances that fragments travelled and wind speed ($R^2 = 0.76$, Fig. 5; Gagnon et al., 2011), while a study by Blackford (1978) found that wind drove up to 50% of the surface currents in the southern Gulf of St. Lawrence. We therefore assumed that wind speed and direction were the best indicators of movement direction of *Codium* fragments, and ignored oceanic currents (as well as tidal currents which act perpendicular to the main direction of spread and likely result in little net movement over long time periods). It should be noted, however, that in offshore areas, oceanic currents can overcome this wind forcing (Blackford, 1978), but as *Codium* is a shallow water species most dispersal occurs along the coast (see Section 4.4.2 for discussion).

Given a dispersal time (T) and fragmentation time (t_0), we calculated the dispersal distance by iteratively tracking a fragment's movement due to wind with a time step of one hour over the dispersal period. Fragmentation times, t_0, were chosen randomly within the month of August, although we examined how spreading speed changed with different fragmentation periods from June to October (see Section 2.7). A fragment's position at time t was calculated as:

$$d_{ij}(t) = d_{ij}(t-1) + \beta_1 v_j(t_0 + t), \tag{7}$$

where $d_{ij}(t)$ is the displacement of fragment i in the NE direction from the location of fragmentation, β_1 is the proportion of the wind speed at which buoyant fragments move (i.e. the slope of the regression in Fig. 5) and $V_j(t)$ is the wind speed to the NW at hour t in year j.

We chose to use wind data from Baccaro Point, Nova Scotia (Fig. 1, Fig. A1.4), as this represents the core area invaded by *Codium* over the past 50 years. Hourly wind speed and direction for Baccaro Point were available online from Environment Canada from 2007 to 2014 (Environment Canada, 2015a), giving us eight different years of wind data. Where hourly wind speeds were missing, we used the linear interpolation between adjacent data points.

2.6. Spread

Thus far, our simulation model tracked the dispersal of buoyant *Codium* fragments accounting for variability in sunlight, fragmentation time and wind speed. However, dispersal potential is only one of several factors determining the invasion success of an introduced species. The species' ability to grow and reproduce in the new environment is also necessary for continued spread, i.e., if fragments do no settle in suitable areas (with available substrate or sufficient sunlight), or if no thalli survive the winter to produce new buoyant fragments, then *Codium* will not spread. We modelled the spread of *Codium* along a one-dimensional coastline as an integro-difference equation for the population (according to Lewis et al., 2006):

$$n(x, t+1) = \sigma n(x, t) + pF(n(x, t)) + \gamma(1-p)\int_{-\infty}^{\infty} k(x-y)F(n(y, t))\,dy, \tag{8}$$

where $n(x, t)$ is the number of the individual thalli at location x and year t, σ is the survival rate of the thalli, γ is the proportion of floating fragments that survive and settle, $F(n)$ is the fragmentation function, $(1-p)$ is proportion of fragments that are buoyant at fragmentation, and $k(x,y)$ is the dispersal function of the fragments, which describes the probability that a fragment disperses from location y to location x. We assumed that the dispersal only depends on the relative distance between locations and wrote $k(x,y)$ as $k(x-y)$.

Let $r = F'(0)$. Then r represents the average number of fragments produced per thallus per year when the total population size is very small. In our simulation, we chose $F(n) = r$ with r being a constant fragmentation rate.

We considered the following equation to study the spreading speed of *Codium* along a one-dimensional domain,

$$n(x, t+1) = \sigma n(x, t) + prn(x, t) + \gamma r(1-p)\int_{-\infty}^{\infty} k(x-y)n(y, t)\,dy, \tag{9}$$

which is the linearization of the above Eq. (8) at $n = 0$ and gives the same spreading speeds as for Eq. (8) (e.g. Kot et al., 1996). Let $M(s) = \int_{-\infty}^{\nu} k(\zeta)e^{s\zeta}\,d\zeta$ be the moment generating function of the dispersal kernel k, where s is the variable of M and can be understood as a measure of the steepness of the wave at the leading edge of the spreading population. According to the theory of spreading speeds for the integro-difference equations (Weinberger, 1982; Kot et al., 1996), the spreading speed to the northeast is:

$$c^{NE} = \min_{s>0} \frac{\ln(\sigma + pr + (1-p)\gamma rM(s))}{s}, \tag{10}$$

and the spreading speed in the southwest direction is:

$$c^{SW} = \min_{s>0} \frac{\ln(\sigma + pr + (1-p)\gamma rM(-s))}{s}. \tag{11}$$

c^{SW} is positive if the spread in the SW direction moves to the south and negative if the spread in the SW direction moves to the north; c^{NE} is positive if the spread in the NE direction moves to the north and negative if the spread in the NE direction moves to the south.

The formulae for the spreading speeds (Eqs. (10) and (11)) assume that the dispersal kernel does not change over time. However, in our case the dispersal kernel differed from year to year due to the stochastic nature of the wind that drives the dispersal of buoyant fragments. This yields a series of dispersal kernels, $k_0, k_1, \ldots, k_t$, where t is the number of years considered. The corresponding moment generating functions are given by $M_0(s), M_1(s), \ldots, M_t(s)$. The spreading speed to the northeast was therefore unlikely to be constant from year to year, but can be considered to be a random variable (Neubert et al., 2000):

$$c_t^{NE} = \min_{s>0} \frac{1}{t}\sum_{j=0}^{t-1} \frac{\ln(\sigma + pr + (1-p)\gamma rM_j(s))}{s}. \tag{12}$$

A similar equation results for the spreading speed to the southwest.

We used an empirical estimator to approximate the moment generating functions $M_j(s)$ based on our mechanistic simulation model of buoyant dispersal. The empirical estimator is:

$$M_j^E(s) = \frac{1}{N}\sum_{i=1}^{N} \exp(sd_{ij}), \tag{13}$$

where N is the number of fragments and d_{ij} is the dispersal distance of fragment i in year j. We simulated these dispersal distances using our dispersal model in a Monte Carlo framework, repeating the simulation for 1000 independent fragments. This number of fragments was enough to reduce most of the variability in spreading speed due to low sample size in the estimation of $M_j(s)$ (Fig. A1.3), while reducing computational time, thus allowing us to perform sensitivity analyses for various parameters. Using the simulation model to generate a large number of d_{ij}, we could use $M_j^E(s)$ to replace $M_j(s)$ in the expressions of c_t^{NE} and c_t^{SW}.

There were eight years of hourly wind data available to us (2007–2014; Environment Canada, 2015a), which is far less than the half-century that *Codium* has been dispersing. We therefore assumed that these eight years of data were representative, and sampled from these eight years with replacement to obtain $t = 0$ dispersal kernels used to calculate $M_j^E(s)$ in Eq. (13). We repeated this sampling 1000 times to obtain a bootstrapped distribution of spreading speeds, from which the mean and 95% quantiles are reported (see *Supplement A3* for the bootstrapping algorithm).

2.6.1. Spread in two-dimensions

We expanded the model to account for dispersal in two dimensions, using the wind speed in all directions rather than just the NE component (*Supplement A4*). This allowed us to consider how winds perpendicular to the coastline might introduce a bias by reducing fragment survival, either blowing some fragments offshore where they will sink in areas too deep to support *Codium* populations, or by blowing fragments onshore. We would expect these biases to be important if there was a correlation in along-shore and cross-shore wind speeds. However, we found that the overall dispersal distances were similar in the one-dimensional and two-dimensional models. The survival of fragments declined as many were blown outside of the settlement zone close to shore, requiring that the trajectories of many more fragments be simulated to obtain a large enough sample of "successful" settlers. Furthermore, the two-dimensional model was computationally more complex, and thus the simulations took much longer to run. We therefore chose to use only the along-shore wind (i.e. NE–SW) to model spread along the NW Atlantic coast, while incorporating fragment survival in the spread model. An example of using the two-dimensional model to simulate dispersal is shown in *Supplement A4*.

2.7. Sensitivity analyses

We were interested in the factors that most influence the population spread of invasive *Codium*. Given the uncertainty in some of our variables, we investigated the sensitivity of spreading speed to different parameters in the model (Fig. 2).

Prior to running simulations, we first investigated the sensitivity of spreading speed to the number of fragments in the IBM, from 10 to 10 000, in order to determine how many fragments to simulate. As mentioned in Section 2.1, we chose 1000 fragments because the estimates of spreading speed did not change with a higher number of fragments (Fig. A1.3).

We then considered how spreading speed changed depending on the month in which fragmentation occurred. The number of daylight hours, probability of a sunny day, and wind data differed from month to month, and likely affected spreading speeds (Table A1). In determining the sensitivity of spreading speed to the time of fragmentation, we considered one-month fragmentation periods that started at the beginning or middle of each month for June through September. This analysis provided insight into how changes in the timing of fragmentation, perhaps due to changes in the timing of storms associated with climate change (Kirtman et al., 2013), may affect the spreading speed of *Codium*.

We also investigated how spreading speed changed over several environmental variables: the probability of a sunny day (α, Section 2.4), well as two variables for which we had little available data and high uncertainty: the proportion of excess oxygen at fragmentation (ω, Section 2.4) and the leakage rate (λ, Section 2.4). These parameters affect the dispersal times, and so for each value that we considered, we simulated dispersal times and bootstrapped 1000 values of the spreading speed (see algorithm in *Supplement A3*). We varied α from 0 to 1 in increments of 0.1, ω from 0.05 to 1 in increments of 0.05, and λ from 0 to 0.2 h^{-1} in increments of 0.01 h^{-1}. When analysing the sensitivity of spreading speed to a particular parameter, all other parameters were held at their base values (Table 1).

For the sub-model for population spread (Section 2.6), we investigated the proportional change in the mean spreading speed, $c_t^{\bar{NE}}$, with changes to each of the four demographic parameters: σ, p, r and γ. This proportional change, termed elasticity, was calculated as the proportional change in the response (i.e. spreading speed) with a 1% change in the parameter of interest in either direction:

$$E_\theta = \frac{c_t^{\bar{NE}}(\theta + 0.01\theta) - c_t^{\bar{NE}}(\theta - 0.01\theta)}{0.02c_t^{\bar{NE}}(\theta)} \tag{14}$$

where θ is the base value of the parameter of interest (σ, p, r or γ; Table 1). We calculated the elasticity to the four demographic parameters over increasing proportion of fragments non-buoyant in order to see how their importance changed as the population dynamics shifted from only reproduction via long-distance buoyant dispersal (i.e., $p = 0$) to only local reproduction (i.e., $p = 1$). We also report the relative importance of each parameter, calculated as $|E_\theta| / \max|E|$, where $\max|E|$ is the maximum absolute value of the elasticities across all four parameters.

3. Results

3.1. Spread

Simulations using environmental data from eastern Canada suggest that buoyant dispersal can drive the spread of *Codium* to the southwest at an average speed of 36.6 km yr^{-1} (95% confidence interval: 35.2–37.9 km yr^{-1}) but only 4.2 km yr^{-1} (3.4–4.9 km yr^{-1}) to the northeast (Fig. A1.2).

The spreading speed depended on the time period when fragmentation was initiated because the number of daylight hours and probability of a sunny day changed from month to month. Fragmentation in June or early July, when there are the most daylight hours, resulted in the longest dispersal times due to greater potential for photosynthesis (Fig. 6A). These long dispersal times resulted in the largest spreading speeds in June, particularly to the southwest (Fig. 6B). When fragmentation occurred in September, spreading speed declined as light was limiting and dispersal times were low.

3.2. Sensitivity analyses

As we increased the probability of a sunny day (α), fragments remained buoyant for a longer time, resulting in longer dispersal times and greater spreading speeds to the south (the dominant

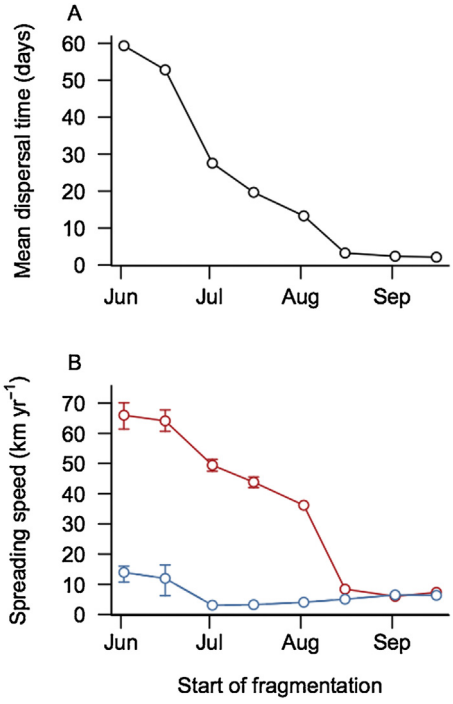

Fig. 6. (A) Mean dispersal time and (B) spreading speeds to the northeast (c^{NE}; blue) and southwest (c^{SW}; red) over eight different one-month fragmentation periods beginning in June through September. Points in (A) are the are the mean and 95% bootstrapped confidence intervals on the mean for the 1000 fragments, and points in (B) are the mean and 95% quantiles of 1000 bootstrapped calculations of the stochastic spreading speed from eight different years of wind data (see Section 2.5). (For interpretation of the references to colour in this figure legend, the reader is referred to the web version of this article.)

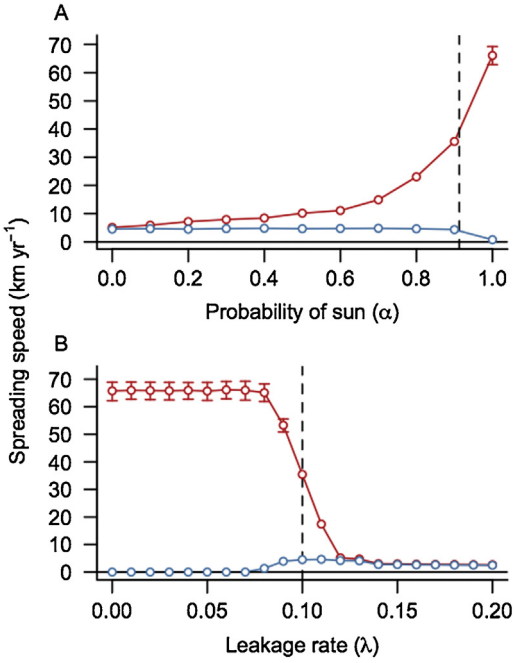

Fig. 7. Sensitivity of spreading speed in the northeast (c^{NE}; blue) and southwest (c^{SW}; red) to (A) the probability of a sunny day (α) and (B) the leakage rate of oxygen from the medulla (λ). Points and error bars are the mean and 95% confidence intervals from1000 bootstrapped calculations of the stochastic spreading speed (see Section 2.6). Vertical dashed line indicates the base parameter values (Table 1). (For interpretation of the references to colour in this figure legend, the reader is referred to the web version of this article.)

wind direction), with maximum spread of 66 km yr^{-1} to the southwest when there was 100% probability of a sunny day (Fig. 7A).

The leakage rate (λ) also had a large effect on spreading speed, especially near the base value of $\lambda = 0.1\ h^{-1}$ (Fig. 7B). Small increases in the leakage rate between values of $\lambda = 0.08\ h^{-1}$ to $\lambda = 0.12\ h^{-1}$ had a large effect on the spreading speed ($c_t^{SW} = 65.1$ km yr^{-1} to $c_t^{SW} = 5.2$ km yr^{-1}). Leakage rates above $0.14\ h^{-1}$ had less of an effect, as dispersal times and therefore spreading speeds approached zero (Fig. 7B).

On the other hand, the proportion of the medulla of a fragment that was filled with oxygen at the time of fragmentation (ω) had little effect on the spreading speed (Fig. A1.3B), likely because the leakage rate and photosynthetic rates were relatively high (Fig. 3B) and therefore much more important than the initial amount of oxygen in the medulla.

3.3. *Elasticity in the spread model*

The fragmentation rate (r) was generally the most important demographic parameter affecting the spread of *Codium* along a one-dimensional coastline (Fig. 8). Higher fragmentation rates resulted in higher spreading speeds in the southwest direction (Fig. 8A). However, when few fragments were buoyant (i.e., $p \approx 1$), the proportion of fragments that were non-buoyant became more important than the fragmentation rate, with small increases in p resulting in large decreases in spreading speed (Fig. 8B).

Interestingly, when the proportion of fragments that were non-buoyant was small (i.e., $p \approx 0$), a small increase in p resulted in an increase in spreading speed (i.e., elasticity was positive; Fig. 8A). This is the opposite of what we had initially expected, given that we proposed buoyant fragments could disperse longer distances and therefore increase spreading speeds. However, by rearranging Eq. (12), it became clear that absolute spreading speed will increase with the proportion of non-buoyant fragments if $\gamma M_j(s) < 1$.

The survival of adult thalli (σ) was relatively unimportant in affecting spreading speed (Fig. 8), likely because in our model these thalli do not contribute to spread except by producing fragments.

4. Discussion

4.1. *Spread of* Codium

We developed a model for the spread of the invasive alga *Codium fragile* in the NW Atlantic that includes the wind-driven dispersal of buoyant fragments. To our knowledge, this is the first attempt at a mechanistic framework for *Codium* dispersal accounting for low-probability long-distance dispersal events that likely drive the front of the invasion (Hastings et al., 2005). Our model showed that prevailing winds are an important determinant of spreading speed of buoyant fragments, and thus prevailing southerly winds on the east coast of Canada in the late summer and autumn are predicted to drive spread southwards at a speed of ~37 km yr^{-1}, while spread towards Newfoundland is predicted to occur much slower at ~ 4 km yr^{-1}. As we used environmental conditions from the northern extent of the invasion, this should indicate that further northward spread by natural means is unlikely under current conditions. Our distribution of spreading speeds was consistent with the theoretical prediction of an asymptotically Gaussian distribution for the stochastic spreading speed over large time intervals (Fig. A1.2; Neubert et al., 2000).

A previous estimate of the spread of *Codium* by Lyons and Scheibling (2009) was based on extrapolating a linear spreading speed from reported sightings of *Codium* along the NW Atlantic coast. They predicted that a strong surface current should be driving *Codium* spread southwards rather than northwards. However, linear regressions of actual spread (based on reported

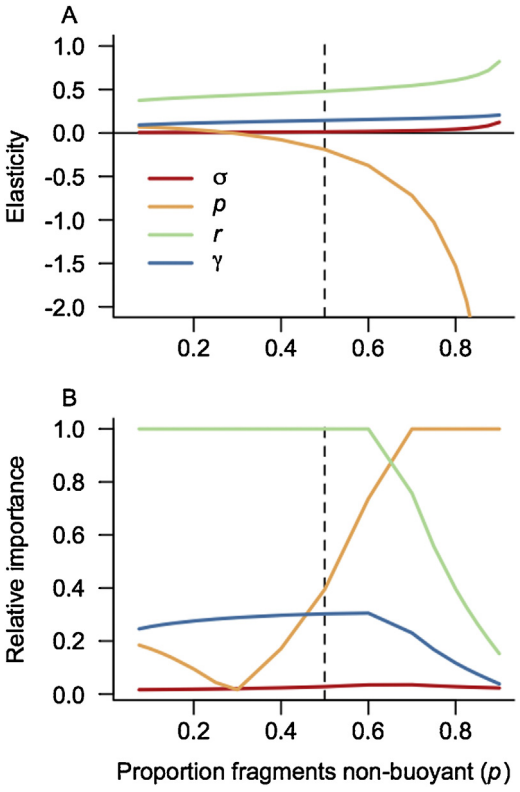

Fig. 8. (A) Elasticity and (B) relative importance of four parameters (coloured lines): the annual survival rate of attached thalli (σ, red), the proportion of fragments that are non-buoyant (i.e., non-dispersing; p, orange), the number of fragments produced per thalli per year (r, green), and the proportion of floating fragments that survive and settle (γ, blue) to the mean spreading speed to the southwest. Vertical dashed line indicates the base value of $p = 0.5$; all other parameters were constant at their base values (Table 1). (For interpretation of the references to colour in this figure legend, the reader is referred to the web version of this article.)

sightings) showed that spread towards the northeast has occurred at 26 ± 3 km yr^{-1}, while spread towards the southwest at a speed of 37 ± 5 km yr^{-1}. They thus concluded that northward spread has mostly occurred due to human-mediated transport, while southward spread is likely due to natural spread (i.e., buoyant fragments), but that oceanic currents were poor predictors for the dispersal of this alga. Local wind conditions are highly variable, but in any case, the general conclusions of both analyses are in agreement (dominant natural spread towards the south, with speed within the same order of magnitude). Similarly, Trowbridge (1998) reported average spread of invasive *Codium* around the world of 65–70 km yr^{-1}, while Kelly et al. (2014) found spread of ~70 km yr^{-1} in Europe, both of which included anthropogenic dispersal but are within the same magnitude as predicted by our model.

While we predicted little northward spread through natural dispersal mechanisms, spread by anthropogenic means is a definite possibility that falls outside the predictions of our model. Much of the spread of *Codium* around the world and in the NW Atlantic seems to have occurred through human-mediated dispersal, either through ship fouling or transport of aquaculture materials (Carlton and Scanlon, 1985; Trowbridge, 1998). Indeed, *Codium* has recently been reported from the southern and eastern coasts of Newfoundland, approximately 500 km east and northeast, respectively, from *Codium* populations in the southern Gulf of St. Lawrence (Matheson et al., 2014). The authors concluded that the introduction of *Codium* into Newfoundland waters was likely anthropogenic, due to the high densities of algae found in areas with high shipping activity, and based on our model we agree – to reach Newfoundland from the southern Gulf of St. Lawrence, fragments would have not only had to disperse in opposite directions than the prevailing wind, but also would have had to cross the Gaspé current (Fig. 1). Here, water velocities are the strongest within the Gulf of St. Lawrence (El-Sabh, 1976) and though the surface current here does not necessarily correlate with wind (Blackford, 1978; see also Section 4.4.2), the prevailing direction is to the southeast, away from Newfoundland.

4.2. Sensitivity of the model to different factors

4.2.1. Fragmentation

The model was especially sensitive to fluctuations in the fragmentation rate (parameter r, i.e., the number of fragments produced), which is in turn determined by the adult population, as well as mechanisms inducing fragmentation. In effect, spreading speed increases as the population size increases, thus leading to an increasing invasion speed over time. In addition to fragments, *Codium* also reproduces via small parthenogenetic propagules, which act to increase local abundance of *Codium* thalli (Trowbridge, 1998). Parthenogenetic reproduction could also contribute to high local population growth, thus increasing the fragmentation rate and spreading speed.

The timing of fragmentation was also an important factor, with fragments produced in June or July having a higher dispersal potential than fragments produced in late autumn. However, since mechanically- and temperature-induced fragmentation is higher in autumn (Fralick and Mathieson, 1972), there is a trade-off between maximum fragmentation rates and maximum dispersal potential.

4.2.2. Proportion of buoyant fragments

We found an interesting interaction between the proportion of fragments that were non-buoyant and the survival of buoyant fragments that dictated the optimal strategy for *Codium* to invade. If the survival of buoyant fragments is very low ($\gamma < 0.013$, using our base parameters in Table 1), *Codium* can spread faster if it invests in local population growth through non-buoyant fragments and the spreading speed actually increase as the proportion of buoyant fragments decrease, though this spreading speed is still much slower than when survival is high. However, if the survival of buoyant fragments is higher, then spreading speed increase as the proportion of buoyant fragments increases.

4.2.3. Physiological aspects

The production and maintenance of oxygen bubbles in the medulla is essential for fragments to maintain buoyancy for long periods of time (>3 days; Gagnon et al., 2011). We found that the rate of oxygen leakage from the medulla (λ) was a key parameter affecting dispersal time and therefore spreading speed. Spreading speed declined exponentially as we increased the rate at which oxygen leaked form the medulla. However, there is very little known about how oxygen bubbles are maintained in the medulla or what might affect leakage of oxygen from the medulla, providing an avenue for future research into long-distance dispersal potential of *Codium*.

4.3. Management implications

As mentioned in Section 4.2.1, the fragmentation rate was the most important factor in determining spread. As fragmentation increases with population, controlling the *Codium* population density would have the highest impact on spread, and this would become more difficult with increased spread. Therefore, any management policies should be put into place early in the invasion process to have a chance at being successful (Meier et al., 2014) as later interventions once the species has become established and started spreading is likely to have limited success and much higher costs. The timing of the interventions is also important, as controlling

populations in early summer would limit the amount of fragments with very high dispersal potential, but control in autumn could decrease the total amount of fragments at a time when fragmentation rates are high. Once a species has spread, compromises in interventions are often required, and therefore our model could help in determining the most effective timing and location of interventions, to prevent further spread (Shea et al., 2010; Meier et al., 2014).

4.3.1. Impacts of climate change

Our estimates of spreading speed were calculated using environmental conditions in eastern Canada over the past decade. However, ongoing climate change is likely to alter many of these conditions, possibly altering the dispersal pathways of many organisms (Travis et al., 2013), including *Codium*. Indeed, Hellmann et al. (2008) listed "altered transport and introduction mechanisms" as the first consequence of climate change for species invasions. For *Codium*, wind and light intensity are the most important environmental conditions determining spread.

Future wind conditions are among the most difficult to predict (Kirtman et al., 2013) as they are highly variable, but an increase in storm frequency is possible due to a northward shift in the storm track. Increasing storm frequency would likely lead to higher summer fragmentation rates of *Codium*, thus improving the timing between the period of peak fragmentation and peak dispersal potential (though this could render the timing of management interventions easier). Increased disturbance rates due to storms could lead to higher settlement success of fragments (e.g. disturbances which clear kelp beds in Nova Scotia have led to population explosions of *Codium* in these areas, see Scheibling and Gagnon, 2006; Watanabe et al., 2010 for more details). However, increased storm frequencies could also decrease light availability for *Codium* in the summer months (either due to more cloudy days, or increased water turbidity), thus somewhat mitigating the impacts of high fragmentation rates.

Increased storm frequency should also render winds more unpredictable, and therefore lead to more switching between wind directions. This may decrease the southward bias of *Codium* spread and allow for more northward natural spread. In addition, juvenile stages of *Codium* seem to require temperatures > 12 °C (Malinowski, 1974; Trowbridge, 1998), which may currently be providing another barrier to further northward spread. Increased sea temperatures of 1–2 °C over the next 20 years (Kirtman et al., 2013) could lead to areas which were previously too cold becoming suitable for the settlement and growth of *Codium*, thus increasing the chances of northward spread.

4.4. Model assumptions and limitations

The mechanistic modelling approach we used in this study aimed to determine the factors controlling long-distance spread of buoyant *Codium* fragments by exploring a range of parameters and environmental conditions. Other work has calculated rates of spread without delving into the mechanisms (e.g. Lyons and Scheibling, 2009) or focused on the mechanisms at a confined scale using field-based observations and experiments (e.g. Watanabe et al., 2009; Gagnon et al., 2011). The modelling approach we took allowed us to bridge these two scales of study by using parameters calculated from previous studies (e.g. Gagnon et al., 2011), available data on environmental conditions (Environment Canada, 2015a, 2015b), and known physical and physiological relationships (Arnold and Murray, 1980). However, our mechanistic modelling approach required us to make assumptions and simplify certain real-world characteristics. In the following sections, we discuss the major assumptions and limitations of our approach.

4.4.1. Geography

We modelled dispersal along a straight coastline, and thus our model also ignores how coastal characteristics such as estuaries, bays, and islands might alter local currents and winds, creating areas where fragments could accumulate (i.e., retention zones) and dispersal would be limited (Largier, 2004; Brennan et al., 2014), but also areas where strong currents and winds could combine to accelerate dispersal speed (Brennan et al., 2014). The one-dimensional model also ignores the role of depth and substrate in the spread of *Codium* (see Sections 2.6.1 and 4.4.2); *Codium* requires shallow water (<3 m) and appropriate substrate (hard substrate or seagrass meadows) to settle and grow (Trowbridge, 1998; Garbary et al., 2004). Thus settlement success will vary according to the local area and characteristics (e.g. settlement success will likely be higher in a large shallow bay than an exposed cliff). Disturbances and the presence of artificial substrates are also important factors that could greatly increase settlement success (Bulleri et al., 2006; Gagnon et al., 2015). For these reasons, the current model should not be used to predict spread at small geographic scales where the above conditions could be more important than wind speeds. However, as mentioned in Section 4.1, our results (at a large scale) are similar to actual observed spreading rates (Lyons and Scheibling, 2009), and in the context of biological invasions, this spread of large scales is generally considered to be the most important in determining the range and impacts of a species (e.g. Hastings et al., 2005). The model could, however, be modified for use in smaller scales if local wind and current directions are known, e.g. to determine how spread varies in different regions and thus how management scenarios should be applied.

4.4.2. Oceanic currents

We also assumed throughout the model that buoyant fragment dispersal was mainly driven by wind as previous experiments showed high correlation between dispersal and wind speed (Gagnon et al., 2015). However, that study took place in coastal lagoons unaffected by oceanic currents. Indeed, in areas where strong oceanic currents occur, surface currents are not correlated with wind speed or direction (e.g. the previous-mentioned Gaspé Current; Blackford, 1978). However, we expect that since *Codium* occurs in shallow waters, dispersal of fragments will be mostly along the coast and in shallow areas, where oceanic currents are less important and thus wind is the primary determinant of surface currents (Blackford, 1978). Supporting this, wind-driven transport of organisms in shallow coastal waters has been previously noted (e.g. Commito et al., 1995; McQuaid and Phillips, 2000). We also ignored any contribution of tidal currents as tides generally act perpendicular to the main direction of spread though they are likely important in determining the survival of buoyant fragments (which depends on settling in appropriate depths and not washing up on shore or in deeper areas, see also previous Section 4.4.1). Wind-driven transport as we considered in this model only applies to buoyant fragments, and future models of spread could incorporate the hydrodynamics that could influence both buoyant and non-buoyant fragments, such as in work modelling the movement of larval fish in networks of marine protected areas (Watson et al., 2011) and the dispersal of parasites in coastal regions of aquaculture (Foreman et al., 2009).

4.4.3. Contribution of other modes of dispersal

As previously mentioned, we only treated dispersal by buoyant fragments in this model, as these are the primary contributors to long-distance dispersal. But *Codium* can also reproduce via small parthenogenetic propagules (Trowbridge, 1998; Stiger and Payri, 1999), small buds, and non-buoyant fragments, which act to increase local population density. Though little is known about the role of these parthenogenetic propagules, Churchill and Moeller

(1972) noted that they swam weakly and settled within 30 minutes, likely limiting their dispersal to several metres from the parent plant. Meanwhile, buds and non-buoyant can disperse several tens of metres, likely contributing to local population growth (Watanabe et al., 1999; Gagnon et al., 2015). While not directly contributing to long-distance dispersal, the role of these types of propagules in spread is likely quite important as high local population growth will greatly increase the fragmentation rate, is an important factor in determining spreading speed (see Section 3.2). The environmental factors determining the dispersal of these non-buoyant propagules are very different from those affect buoyant fragments, and are usually linked to physical characteristics of the substrate and bottom currents (Watanabe et al., 2009; Gagnon et al., 2015), therefore cannot be accounted for in our model. Models for the dispersal of non-buoyant algal propagules do exist (e.g. Gaylord et al., 2002, 2006), though *Codium* is not one of the species modelled). The aforementioned models take into account such factors as release height about the bottom, sinking speed, currents and wave forces, and could potentially be modified and combined with information on substrate characteristics to form a complete picture of both short and long-distance dispersal for *Codium*.

5. Conclusions

Previous studies on the dispersal of an invasive species such as *Codium* have often been based on reported sightings of the species over time an assumed a constant spreading speed. However, Hastings et al. (2005) suggested that rare long-distance dispersal events may be more important than local population growth in driving the secondary spread of an invasive species. By incorporating a mechanistic model for buoyancy, we modelled the long-distance dispersal of *Codium* fragments via buoyant fragments, and were able to predict the direction and scale of future spread. In doing this, we found that long-distance dispersal via buoyant fragments predicts a pattern of spread that is consistent with historical observations. Environmental factors (i.e., sunlight and wind) and the production rate of buoyant fragments may influence spreading speed more than local population growth or the survival of adult thalli. Secondary spread may therefore be strongly affected by changes to wind direction and storm intensity associated with global warming.

In addition, we identified several parameters that are still relatively unknown (i.e., the rate of oxygen leakage from the thallus may strongly influence dispersal potential, but little is known about this phenomenon). Further research is thus needed into the buoyant properties of *Codium* with respect to long-distance dispersal capabilities (Gagnon et al., 2011).

Though we applied our model to simulate spread in eastern Canada, this model could also be applied to *Codium* in other areas around the world where it has invaded. With some modifications, the model could also be applied to predict the spread of other invasive buoyant algae (e.g. *Undaria pinnatifida*; Forrest et al., 2000) or important native species (e.g. *Zostera marina*; Harwell and Orth, 2002), which spread through both buoyant and non-buoyant propagules. In particular, this model could be particularly useful to quantify the contribution of long-distance dispersal events, which, though rare, tend to determine spreading speed. For the invasive species, this model could be used to determine appropriate management strategies to decrease spread, while for threatened or important native species, it could contribute to planning more effective protective measures, such as marine protected areas.

Acknowledgements

We are grateful to Ladd Johnson for guidance regarding the field components of the *Codium* research and for encouragement to undertake this modelling project. We also thank two anonymous reviewers for their comments, which greatly improved the quality of this manuscript. This work was supported by Canadian Aquatic Invasive Species Network (CAISN), a network of the Natural Sciences and Engineering Research Council (NSERC) funding to K.G. and M.A.L., an Alberta Ingenuity Postgraduate Scholarship and NSERC Vanier Scholarship to S.J.P., MITACS Network for Biological Invasions and Dispersal, NSERC, Sustainable Resource Development Alberta, and Alberta Water Research Institute funding to Y.J., and NSERC Discovery and Accelerator Grants, a Killam Research Fellowship and a Canada Research Chair to M.A.L.

Appendix A. Supplementary data

Supplementary data associated with this article can be found, in the online version, at http://dx.doi.org/10.1016/j.ecolmodel.2015.08.011.

References

Arnold, K.E., Murray, S.N., 1980. Relationships between irradiance and photosynthesis for marine benthic green algae (Chlorophyta) of differing morphologies. J. Exp. Mar. Biol. Ecol. 43, 183–192, http://dx.doi.org/10.1016/0022-0981(80)90025-8.

Bégin, C., Scheibling, R.E., 2003. Growth and survival of the invasive green alga *Codium fragile* ssp. *tomentosoides* in tide pools on a rocky shore in Nova Scotia. Bot. Mar. 46, 404–412, http://dx.doi.org/10.1515/BOT.2003.040.

Blackford, B.L., 1978. Wind-driven inertial currents in the Magdalen Shallows, Gulf of St. Lawrence. J. Phys. Oceanogr. 8, 653–664, doi:10.1175/1520-0485(1978)008<0653:WDICIT>2.0.CO;2.

Blakeslee, A.M.H., McKenzie, C.H., Darling, J.A., Byers, J.E., Pringle, J.M., Roman, J., 2010. A hitchhiker's guide to the Maritimes: anthropogenic transport facilitates long-distance dispersal of an invasive marine crab to Newfoundland. Divers. Distrib. 16, 879–891, http://dx.doi.org/10.1111/j.1472-4642.2010.00703.x.

Bouck, G.B., Morgan, E., 1957. The occurrence of *Codium* in Long Island waters. Bull. Torrey Bot. Club 84, 384–387, http://dx.doi.org/10.2307/2483114.

Brennan, G., Kregting, L., Beatty, G.E., Cole, C., Elsasser, B., Savidge, G., Provan, J., 2014. Understanding macroalgal dispersal in a complex hydrodynamic environment: a combined population genetic and physical modelling approach. J. R. Soc. Interface 11, 20140197, http://dx.doi.org/10.1098/rsif.2014.0197.

Bulleri, F., Abbiati, M., Airoldi, L., 2006. The colonisation of human-made structures by the invasive alga *Codium fragile* ssp. *tomentosoides* in the north Adriatic Sea (NE Mediterranean). Hydrobiologia 555, 263–269, http://dx.doi.org/10.1007/s10750-005-1122-4.

Carlton, J.T., Scanlon, J.A., 1985. Progression and dispersal of an introduced alga: *Codium fragile* ssp. *tomentosoides* (Chlorophyta) on the Atlantic coast of North America. Bot. Mar. 28, 155–1665, http://dx.doi.org/10.1515/botm.1985.28.4.155.

Chapman, A.S., 1999. From introduced species to invader: what determines variation in the success of *Codium fragile* ssp. *tomentosoides* (Chlorophyta) in the North Atlantic Ocean? Helgolander. Meeresun. 52, 277–289, http://dx.doi.org/10.1007/BF02908902.

Churchill, A.C., Moeller, H.W., 1972. Seasonal patterns of reproduction in New York populations of *Codium fragile* (Sur.) Hariot subsp. *tomentosoides* (van Goor) Silva. J. Phycol. 8, 147–152, http://dx.doi.org/10.1111/j.1529-8817.1972.tb04016.x.

Commito, J.A., Thrush, S.F., Pridmore, R.D., Hewitt, J.E., Cummings, V.J., 1995. Dispersal dynamics in a wind-driven benthic system. Limnol. Oceanogr. 40, 1513–1518, http://dx.doi.org/10.4319/lo.1995.40.8.1513.

DeAngelis, D.L., Mooij, W.M., 2005. Individual-based modeling of ecological and evolutionary processes. Annu. Rev. Ecol. Evol. Syst. 36, 147–168, http://dx.doi.org/10.1146/annurev.ecolsys.36.102003.152644.

Deysher, L., Norton, T.A., 1982. Dispersal and colonization in *Sargassum muticum* (Yendo) Fensholt. J. Exp. Mar. Biol. Ecol. 56, 179–195, http://dx.doi.org/10.1016/0022-0981(81)90188-X.

Dromgoole, F.I., 1982. The buoyant properties of *Codium*. Bot. Mar. 25, 391–397, http://dx.doi.org/10.1515/botm.1982.25.8.391.

El-Sabh, M.I., 1976. Surface circulation pattern in the Gulf of St. Lawrence. J. Fish. Res. Board Can. 33, 124–138, http://dx.doi.org/10.1139/f76-015.

Environment Canada, 2015a. Hourly wind speed and direction for Baccaro Point, NS from 2007–2014, Accessed 23 March 2015 from http://climate.weather.gc.ca/index_e.html

Environment Canada, 2015b. Climate normals for Sydney, NS from 1981–2000, Accessed 23 March 2015 from http://climate.weather.gc.ca/climate_normals/index_e.html

Fennell, M., Murphy, J.E., Armstrong, C., Gallagher, T., Osborne, B., 2012. Plant spread simulator: a model for simulating large-scale directed dispersal processes across heterogeneous environments. Ecol. Model. 230, 1–10, http://dx.doi.org/10.1016/j.ecolmodel.2012.01.008.

Fisher, R.A., 1937. The wave of advance of advantageous genes. Ann. Eug. 7, 355–369, http://dx.doi.org/10.1111/j.1469-1809.1937.tb02153.x.

Foreman, M.G.G., Czajko, P., Stucchi, D.J., Guo, M., 2009. A finite volume model simulation for the Broughton Archipelago, Canada. Ocean Model. 30, 29–47, http://dx.doi.org/10.1016/j.ocemod.2009.05.009.

Forrest, B.M., Brown, S.N., Taylor, M.D., Hurd, C.L., Hay, C.H., 2000. The role of natural dispersal mechanisms in the spread of *Undaria pinnatifida* (Laminariales, Paeophyceae). Phycologia 39, 547–553, http://dx.doi.org/10.2216/i0031-8884-39-6-547.1.

Fralick, R.A., Mathieson, A.C., 1972. Winter fragmentation of *Codium fragile* (Suringar) Hariot ssp. *tomentosoides* (van Goor) Silva (Chlorophyceae, Siphonales) in New England. Phycologia 11, 67–70, http://dx.doi.org/10.2216/i0031-8884-11-1-67.1.

Gagnon, K., McKindsey, C.W., Johnson, L.E., 2011. Dispersal potential of invasive algae: the determinants of buoyancy in *Codium fragile* ssp. *fragile*. Mar. Biol. 158, 2449–2458, http://dx.doi.org/10.1007/s00227-011-1746-z.

Gagnon, K., McKindsey, C.W., Johnson, L.E., 2015. Roles of dispersal mode, recipient environment and disturbance in the secondary spread of the invasive seaweed *Codium fragile*. Biol. Invasions 17, 1123–1136, http://dx.doi.org/10.1007/s10530-014-0782-2.

Garbary, D.J., Vandermeulen, H., Kim, K.Y., 1997. *Codium fragile* ssp. *tomentosoides* (Chlorophyta) invades the Gulf of St Lawrence, Atlantic Canada. Bot. Mar. 40, 537–540, http://dx.doi.org/10.1515/botm.1997.40.1-6.537.

Garbary, D.J., Fraser, S.J., Hubbard, C., Kim, K.Y., 2004. *Codium fragile*: rhizomatous growth in the *Zostera* thief of eastern Canada. Helgoland. Mar. Res. 58, 141–146, http://dx.doi.org/10.1007/s10152-004-0173-7.

Gardner, R.H., Gustafson, E.J., 2004. Simulating dispersal of reintroduced species within heterogeneous landscapes. Ecol. Model. 171, 339–358, http://dx.doi.org/10.1016/j.ecolmodel.2003.08.008.

Gaylord, B., Reed, D.C., Raimondi, P.T., Washburn, L., McLean, S.R., 2002. A physically based model of macroalgal spore dispersal in the wave and current-dominated nearshore. Ecology 83, 1239–1251, http://dx.doi.org/10.1890/0012-9658(2002)083[1239:APBMOM]2.0.CO;2.

Gaylord, B., Reed, D.C., Raimondi, P.T., Washburn, L., 2006. Macroalgal spore dispersal in coastal environments: mechanistic insights revealed by theory and experiment. Ecol. Monogr. 76, 481–502, http://dx.doi.org/10.1890/0012-9615(2006)076[0481:MSDICE]2.0.CO;2.

Harwell, M.C., Orth, R.J., 2002. Long-distance dispersal potential in a marine macrophyte. Ecology 83, 3319–3330, http://dx.doi.org/10.2307/3072082.

Hastings, A., Cuddington, K., Davies, K.F., Dugaw, C.J., Elmendorf, S., Freestone, A., Harrison, S., Holland, M., Lambrinos, J., Malvadkar, U., Melbourne, B.A., Moore, K., Taylor, C., Thomson, D., 2005. The spatial spread of invasions: new developments in theory and evidence. Ecol. Lett. 8, 91–101, http://dx.doi.org/10.1111/j.1461-0248.2004.00687.x.

Hellmann, J.J., Byers, J.E., Bierwagen, B.G., Dukes, J.S., 2008. Five potential consequences of climate change for invasive species. Conserv. Biol. 22, 534–543, http://dx.doi.org/10.1111/j.1523-1739.2008.00951.x.

Hengeveld, R., 1989. Dynamics of Biological Invasions. Chapman and Hall, London.

Hwang, E.K., Baek, J.M., Park, C.S., 2008. Cultivation of the green alga *Codium fragile* (Suringar) Hariot, by artificial seed production in Korea. J. Appl. Phycol. 20, 469–475, http://dx.doi.org/10.1007/s10811-007-9265-5.

Kelly, R., Lundy, M.G., Mineur, F., Harrod, C., Maggs, C.A., Humphries, N.E., Sims, D.W., Reid, N., 2014. Historical data reveal power-law dispersal patterns of invasive aquatic species. Ecography 37, 581–590, http://dx.doi.org/10.1111/j.1600-0587.2013.00296.x.

Kirtman, B., Power, S.B., Adedoyin, J.A., Boer, G.J., Bojariu, R., Camilloni, I., Doblas-Reyes, F.J., Fiore, A.M., Kimoto, M., Meehl, G.A., Prather, M., Sarr, A., Schär, C., Sutton, R., van Oldenborgh, G.J., Vecchi, G., Wang, H.J., 2013. Near-term climate change: projections and predictability. In: Stocker, T.F., Qin, D., Plattner, G.-K., Tignor, M., Allen, S.K., Boschung, J., Nauels, A., Xia, Y., Bex, V., Midgley, P.M. (Eds.), Climate Change 2013: The Physical Science Basis. Contribution of Working Group I to the Fifth Assessment Report of the Intergovernmental Panel on Climate Change. Cambridge University Press, Cambridge, United Kingdom and New York, NY, USA, pp. 953–1028.

Kot, M., Lewis, M.A., van den Driessche, P., 1996. Dispersal data and the spread of invading organisms. Ecology 77, 2027–2042, http://dx.doi.org/10.2307/2265698.

Largier, J., 2004. The importance of retention zones in the dispersal of larvae. In: Shipley, J.B. (Ed.), American Fisheries Society Symposium. , pp. 105–122.

Lewis, M.A., Neubert, M.G., Caswell, H., Clark, J., Shea, K., 2006. A guide to calculating discrete-time invasion rates from data. In: Cadotte, M., McMahon, S., Fukami, T. (Eds.), Conceptual Ecology and Invasion Biology: Reciprocal Approaches to Nature. Springer Netherlands, pp. 169–192.

Lyons, D.A., Scheibling, R.E., 2009. Range expansion by invasive marine algae: rates and patterns of spread at a regional scale. Divers. Distrib. 15, 762–775, http://dx.doi.org/10.1111/j.1472-4642.2009.00580.x.

Malinowski, K.C., (Ph.D. Thesis) 1974. *Codium fragile* – the ecology and population biology of a colonizing species. Yale University, New Haven, CT, USA.

Matheson, K., McKenzie, C., Sargent, P., Hurley, M., Wells, T., 2014. Northward expansion of the invasive green algae *Codium fragile* spp. *fragile* (Suringar) Hariot, 1889 into coastal waters of Newfoundland, Canada. Bioinvasions Rec. 3, 151–158, http://dx.doi.org/10.3391/bir.2014.3.3.03.

McQuaid, C.D., Phillips, T.E., 2000. Limited wind-driven dispersal of intertidal mussel larvae: in situ evidence from the plankton and the spread of the invasive species *Mytilus galloprovincialis* in South Africa. Mar. Ecol. Prog. Ser. 201, 211–220, http://dx.doi.org/10.3354/meps201211.

Meier, E.S., Dullinger, S., Zimmermann, N.E., Baumgartner, D., Gattringer, A., Hülber, K., 2014. Space matters when defining effective management for invasive plants. Divers. Distrib. 20, 1029–1043, http://dx.doi.org/10.1111/ddi.12201.

Molnar, J.L., Gamboa, R.L., Revenga, C., Spalding, M.D., 2008. Assessing the global threat of invasive species to marine biodiversity. Front. Ecol. Environ. 6, 485–492, http://dx.doi.org/10.1890/070064.

Neubert, M.G., Caswell, H., 2000. Demography and dispersal: calculation and sensitivity analysis of invasion speed for structured populations. Ecology 81, 1613–1628, http://dx.doi.org/10.1890/0012-9658(2000)081[1613:DADCAS]2.0.CO;2.

Neubert, M.G., Kot, M., Lewis, M.A., 2000. Invasion speeds in fluctuating environments. Proc. R. Soc. B: Biol. Sci. 267, 1603–1610, http://dx.doi.org/10.1098/rspb.2000.1185.

Padilla, D.K., Chotkowski, M.A., Buchan, L.A.J., 1996. Predicting the spread of zebra mussels (*Dreissena polymorpha*) to inland waters using boater movement patterns. Global Ecol. Biogeogr. 5, 353–359, http://dx.doi.org/10.2307/2997590.

Parker, I.M., Simberloff, D., Lonsdale, W.M., Goodell, K., Wonham, M., Kareiva, P.M., Williamson, M.H., Von Holle, B., Moyle, P.B., Byers, J.E., 1999. Impact: toward a framework for understanding the ecological effects of invaders. Biol. Invasions 1, 3–19, http://dx.doi.org/10.1023/A:1010034312781.

Prince, J.S., Trowbridge, C.D., 2004. Reproduction in the green macroalga *Codium* (Chlorophyta): characterization of gametes. Bot. Mar. 47, http://dx.doi.org/10.1515/BOT.2004.062.

Scheibling, R.E., Gagnon, P., 2006. Competitive interactions between the invasive green alga *Codium fragile* ssp. *tomentosoides* and native canopy-forming seaweeds in Nova Scotia (Canada). Mar. Ecol. Prog. Ser. 325, 1–14, http://dx.doi.org/10.3354/meps325001.

Shea, K., Jongejans, E., Skarpaas, O., Kelly, D., Sheppard, A.W., 2010. Optimal management strategies to control local population growth or population spread may not be the same. Ecol. Appl. 20, 1148–1161, http://dx.doi.org/10.1890/09-0316.1.

Shigesada, N., Kawasaki, K., Takeda, Y., 1995. Modelling stratified diffusion in biological invasions. Am. Nat. 146, 229–251, http://dx.doi.org/10.1086/285796.

Simard, N., Paille, N., McKindsey, C.W., 2007. *Codium fragile* ssp. *tomentosoides*: revue de littérature et situation aux Îles-de-la-Madeleine. Can. Manuscr. Rep. Fish Aquat. Sci. 2786, vii+39 p.

Skellam, J.G., 1951. Random dispersal in theoretical populations. Biometrika 38, 196–218, http://dx.doi.org/10.1093/biomet/38.1-2.196.

Stewart, H.L., 2006. Ontogenetic changes in buoyancy, breaking strength, extensibility, and reproductive investment in a drifting macroalga *Turbinaria ornata* (Phaeophyta). J. Phycol. 42, 43–50, http://dx.doi.org/10.1111/j.1529-8817.2006.00184.x.

Stiger, V., Payri, C.E., 1999. Spatial and temporal patterns of settlement of the brown macroalgae *Turbinaria ornata* and *Sargassum mangarevense* in a coral reef on Tahiti. Mar. Ecol. Prog. Ser. 191, 91–100, http://dx.doi.org/10.3354/meps191091.

Travis, J.M.J., Delgado, M., Bocedi, G., Baguette, M., Bartoń, K., Bonte, D., Boulangeat, I., Hodgson, J.A., Kubisch, A., Penteriani, V., Saastomoinen, M., Stevens, V.M., Bullock, J.M., 2013. Dispersal and species' responses to climate change. Oikos 122, 1532–1540, http://dx.doi.org/10.1111/j.1600-0706.2013.00399.x.

Trowbridge, C.D., 1998. Ecology of the green macroalga *Codium fragile* (Suringar) Hariot 1889: invasive and non-invasive subspecies. Oceanogr. Mar. Biol. 36, 1–64.

Vander Zanden, M.J., Olden, J.D., 2008. A management framework for preventing the secondary spread of aquatic invasive species. Can. J. Fish. Aquat. Sci. 65, 1512–1522, http://dx.doi.org/10.1139/F08-099.

Watanabe, S., Metaxas, A., Scheibling, R.E., 2009. Dispersal potential of the invasive green alga *Codium fragile* ssp. *fragile*. J. Exp. Mar. Biol. Ecol. 381, 114–125, http://dx.doi.org/10.1016/j.jembe.2009.09.012.

Watanabe, S., Scheibling, R.E., Metaxas, A., 2010. Contrasting patterns of spread in interacting invasive species: *Membranipora membranacea* and *Codium fragile* off Nova Scotia. Biol. Invasions 12, 2329–2342, http://dx.doi.org/10.1007/s10530-009-9647-5.

Watson, J.R., Siegel, D.A., Kendall, B.E., Mitarai, S., Rassweiller, A., Gaines, S.D., 2011. Identifying critical regions in small-world marine metapopulations. Proc. Natl. Acad. Sci. 108, E907–E913, http://dx.doi.org/10.1073/pnas.1111461108.

Weinberger, H.F., 1982. Long-time behavior of a class of biological models. SIAM J. Math. Anal. 13, 353–396, http://dx.doi.org/10.1137/0513028.

West, E.J., Barnes, P.B., Wright, J.T., Davis, A.R., 2007. Anchors aweigh: fragment generation of invasive *Caulerpa taxifolia* by boat anchors and its resistance to desiccation. Aquat. Bot. 87, 196–202, http://dx.doi.org/10.1016/j.aquabot.2007.06.005.